NASA TECHNICAL MEMORANDUM

NASA TM X-73615

NASA TM X-73615

(NASA-TM-X-73615) BOILING INCIPIENCE AND CONVECTIVE BOILING OF NEON AND NITROGEN (NASA) 18 p HC A02/MF A01 CSCL 20L

N77-28330

Unclas
G3/31 39293

BOILING INCIPIENCE AND CONVECTIVE BOILING OF NEON AND NITROGEN

by S. S. Papell and R. C. Hendricks
Lewis Research Center
Cleveland, Ohio 44135

TECHNICAL PAPER to be presented at the
Joint Meeting of the Cryogenic Engineering Conference
and the International Cryogenic Material Conference
Boulder, Colorado, August 2-5, 1977

BOILING INCIPIENCE AND CONVECTIVE BOILING OF NEON AND NITROGEN

by S. S. Papell and R. C. Hendricks

National Aeronautics and Space Administration
Lewis Research Center
Cleveland, Ohio 44135

ABSTRACT

Forced convection and subcooled boiling heat transfer data for liquid nitrogen and liquid neon were obtained in support of a design study for a 30 tesla cryomagnet cooled by forced convection of liquid neon. This design precludes nucleate boiling in the flow channels as they are too small to handle vapor flow. Consequently, it was necessary to determine boiling incipience under the operating conditions of the magnet system.

The cryogen data obtained over a range of system pressures, fluid flow rates, and applied heat fluxes were used to develop correlations for predicting boiling incipience and convective boiling heat transfer coefficients in uniformly heated flow channels. The accuracy of the correlating equations was then evaluated.

A technique was also developed to calculate the position of boiling incipience in a uniformly heated flow channel. Comparisons made with the experimental data showed a prediction accuracy of ±15 percent.

INTRODUCTION

The data reported herein were obtained in support of a design study for a 30 tesla cryomagnet described in reference 1. Because the coolant channels of the magnet coils are too small to handle vapor flow, it was

STAR category 34

necessary to determine boiling incipience and convective boiling coefficients under the operating conditions of the magnet system. Forced convection heat transfer data obtained for this design were correlated and are presented in reference 2.

In spite of the voluminous literature on boiling heat transfer, the predictability of boiling incipience and convective boiling in flowing heat transfer systems is still quite limited. Available empirical and semi-empirical techniques (presented in refs. 3, 4, 5) are mostly derived from water data. In this report we extend these data to liquid neon and liquid nitrogen.

The convective boiling data were correlated by a technique similar to that of reference 5. In addition, the position of boiling incipience in the heated channel was calculated from the value of the correlation parameter at the incipient boiling point. Comparisons were then made with the experimental data.

NOMENCLATURE

A	area, cm^2
C_p	specific heat, J/g-K
C_1 to C_5	constants in eq. (1)
d	diameter, cm
G	$\rho_b V_b = \dot{\omega}/A$
H	enthalpy, J/g
h	heat transfer coefficient, W/cm^2 - K
k	thermal conductivity, J/sec-cm-K
L	distance along test section, cm
Nu	Nusselt number, hd/k
Pr	Prandtl number, $C_p \mu/k$
p	pressure, MPa bars

Q total heat input, W

q heat flux, W/cm^2

Re Reynolds number, $\rho Vd/\mu$

T temperature, K

V velocity, cm/sec

x_i heated length for boiling incipience, cm

λ heat of vaporization, J/g

μ viscosity, g/cm-sec

ρ density, g/cm^3

$\dot{\omega}$ mass flow rate, g/sec

Subscripts

b bulk fluid

boil boiling

calc calculated

fc forced convection

ht heat transfer

in inlet

l liquid

s saturated

v vapor

w wall

APPARATUS AND PROCEDURE

The entire heat transfer apparatus, composed of the cryogen tank, test section, and radiation shield, was housed in a steel vacuum tank (fig. 1). The instrumented test section, designed to simulate the small flow channels

of the proposed liquid neon cooled magnet, was installed to permit vertically upward flow and was uniformly joule heated. Pressurization of a cryogenic supply tank or "blowdown" was used to force the fluid to flow through the test section.

The joule heated Inconel test section was 25 cm long by 0.198 cm i.d. and 0.256 o.d. with a resistance of about 0.148 Ω. An ac power supply provided up to 6.8 V across the test section for a maximum heat flux of 21.2 W/cm^2. Tube wall temperature measurements were made with 40 gage Chromel-constantan thermocouples located at positions 5.7, 8.2, 10.7, 13.3, 15.7, 18.2, 20.7, and 23.1 cm from the test-section inlet-side electrode. The thermocouples were referenced to the fluid temperature in the inlet mixing chamber. Fluid temperatures at the entrance and exit of the test section and in the cryogen tank were measured using platinum resistance thermometers. Mixing chamber pressure taps were provided for pressure measurements. The flow rate was determined by using an orifice in conjunction with measurements of local temperature and pressure near the bottom of the dip tube in the cryogen tank as shown schematically in figure 1.

Before taking any cryogenic data, the flow system and instrumentation accuracy of the test rig were initially checked by taking gaseous nitrogen, neon, and helium heat transfer data. The forced convection heat transfer behavior of these gases is well known, so the experimental heat transfer coefficients from these tests provided adequate information to judge the reliability of the instrumentation. Since these results were within ±10 percent of predictions by the Dittus-Boelter equation the system was considered operational.

With liquid cryogens as the working fluid, the cooldown procedure was tailored to the type of fluid used. When the working fluid was liquid nitrogen, the flow system was initially cooled by the fluid itself. Liquid neon, on the other hand, is too costly to be used as a cooldown fluid. To minimize boiloff losses, the rig was precooled to approximately 20 K with cold helium gas before any transfer of liquid neon was made.

The test procedure required control of system pressure, flow rate, and heat input. After the initial cooldown, the supply tank was filled with the cryogen and then pressurized. The pressurizing gas, either helium or neon,

was also precooled to approximately 80 K with liquid nitrogen to minimize heat transfer to the working fluid. The system pressure and flow rate were set by control of the inlet and outlet valves. At each power setting, time was allowed for the system to reach steady-state conditions before the data were recorded. The same procedure was repeated over a range of flow rates and system pressures.

FORCED CONVECTIVE BOILING CORRELATION

Papell (ref. 5) found the relationship

$$\frac{h_{boil}}{h_{fc}} = C_1 \left[\left(\frac{q\rho_b}{\lambda G \rho_v} \right)^{C_2} \left(\frac{\lambda}{H_s - H_b} \right)^{C_3} \left(\frac{\rho_v}{\rho_l} \right)_s^{C_4} \right]^{C_5} \tag{1}$$

to be effective in the correlation of subcooled boiling water data when the equation constants were $C_1 = 90$, $C_2 = 1.0$, $C_3 = 1.2$, $C_4 = 1.08$, and $C_5 = 0.7$. Preliminary data have shown that for liquid nitrogen and liquid neon modification of this relationship is required.

Liquid Nitrogen Data

The liquid nitrogen data are presented in figure 2 in terms of the ratio of boiling to nonboiling heat transfer coefficients (h_{boil}/h_{fc}) plotted as a function of the three dimensionless parameters of equation (1):

$$\left(\frac{q\rho_b}{\lambda G \rho_v} \right)^{C_2} \left(\frac{\lambda}{H_s - H_b} \right)^{C_3} \left(\frac{\rho_v}{\rho_l} \right)_s^{C_4} \tag{2}$$

An analysis of the data showed a best fit was obtained when C_4 was changed to 1.4 with C_2 and C_3 remaining the same as for the water data. In addition, the forced convection heat transfer coefficient (h_{fc}) in equation (1) was calculated from a Dittus-Boelter type correlation that has been verified in reference 3 for both liquid nitrogen and liquid neon as

$$Nu_{fc} = 0.023(Re)^{0.8}(Pr)^{0.4} \tag{3}$$

with fluid properties at bulk temperature conditions.

The data in figure 2 cover a range of test conditions that include system pressures from 1.11 to 2.87 MPa (11.1 to 28.7 bars), flow rates from 2.7 to 6.5 g/sec, heat flux from 4.1 to 21.2 W/cm^2, and subcooling temperature differentials up to 26.5 K.

Figure 2 shows that the data fall along a line with a slope of 0.7, which is the same slope as the reference 5 water data correlation. An analysis of the scatter shows that 88 percent of the data lie within ±10 percent of the correlating line. The constant C_1 equal to 100 fits the data and the final correlation becomes

$$\frac{h_{boil}}{h_{fc}} = 100\left[\left(\frac{q\rho_b}{\lambda G\rho_v}\right)\left(\frac{\lambda}{H_s - H_b}\right)^{1.2}\left(\frac{\rho_v}{\rho_l}\right)_s^{1.4}\right]^{0.7} \tag{4}$$

The ratio h_{boil}/h_{fc} is a direct indication of the enhanced heat transfer properties of boiling to nonboiling. On figure 2 this ratio remains at a value of unity for all the nonboiling data and is greater than unity when boiling exists. Equation (4) is limited to subcooled boiling because the parameter $(\lambda/H_s - H_b)$ becomes undefined as the bulk fluid becomes saturated. Data with $1\frac{1}{2}$ degree K of saturated bulk conditions were not used because of excessive scatter.

A frequent problem associated with data correlation is the suppression of significant information. Correlations involving exponential terms tend to suppress the scatter of the data employed in developing the correlation equations. Consequently, appreciable uncertainties emerge when the correlation is used

to predict the effect of varying a parameter in the correlation. To test the accuracy of the data correlation to predict h given q, $\dot{\omega}$, and bulk conditions, equation (4) was used to compare calculated and experimental values of heat transfer coefficient ratios. The results (presented in fig. 3) show that 82 percent of the data fall within a ±10 percent scatter. The calculation of heat transfer coefficients from q, $\dot{\omega}$, and bulk conditions is therefore considered reasonably valid, with minor suppression of information.

On the other hand, the calculation of heat flux (q) suffers because of its high dependence on temperature difference. * In order to determine the sensitivity of q_{calc}, equation (4) was reformulated as a function of ΔT, $\dot{\omega}$, and bulk conditions:

$$q_{calc} = \left[100 h_{fc}(T_w - T_b)\right]^{3.33} \left[\left(\frac{\rho_b}{\lambda G \rho_v}\right)\left(\frac{\lambda}{H_s - H_b}\right)^{1.2}\left(\frac{\rho_v}{\rho_l}\right)_s^{1.4}\right]^{2.33} \tag{5}$$

The heat flux was then calculated using equation (5) and compared with the experimental data. The results, presented in figure 4, show a data scatter of ±30 percent. Thus, the sensitivity of the heat flux calculation in equation (4) is about three times greater than that of the heat transfer coefficient ratio calculation.

Liquid Neon Data

Figures 5, 6, and 7 treat the liquid neon data in the same manner as the liquid nitrogen data. Figure 5 shows the correlation of neon data over a range of pressures from 1.12 to 1.66 MPa (11.2 to 16.6 bars), flow rates from 4.0 to 10.8 g/sec, heat flux from 1.8 to 20.5 W/cm^2, and subcooling differentials up to 11.6 K. An analysis shows that 82 percent of the data lies within

---

*By analogy, the sensitivity is quite similar to that in pool boiling where $q \propto \Delta T^3$.

±15 percent of correlation equation (4). The suppression of information (discussed in the Liquid Nitrogen Data section) by this correlation, as determined by comparisons between calculated and experimental heat transfer coefficient ratios, is shown in figure 6. For a given set of q, $\dot{\omega}$, and bulk conditions, approximately 75 percent of the neon data lie within a scatter of ±15 percent. The increased scatter in the neon data over the nitrogen data is partially due to the difference in temperature measurement accuracy. Temperature differences used in the correlation for liquid neon were about half the values obtained for nitrogen. In addition, less stable operation of the rig was noted when using neon rather than nitrogen. It is not understood, at this time, whether the instability was thermally or hydrodynamically driven.

For a given ΔT, $\dot{\omega}$, and bulk conditions, the calculated heat flux using equation (5) is compared with experimental data in figure 7. An analysis shows that the data spread is about ±40 percent which again represents considerable suppression of information.

BOILING INCIPIENCE

The methods available in the literature to predict boiling incipience are described in references 3, 4, and 6. They require information such as the amount of superheat needed to initiate boiling or a knowledge of the bubble site cavity dimensions and the laminar sublayer thickness. All these parameters are functions of test conditions and are not readily available for most fluids.*

The boiling correlation technique presented herein is premised on commercial tubes and can be used to determine local bulk enthalpy and density conditions at boiling incipience for both liquid nitrogen and liquid neon. These local conditions can then be used to calculate the position of boiling incipience in the heated channel.

---

*We do not mean to imply that sites, sublayers, etc., are not important to the mechanism of nucleate boiling - only that for a given geometry they vary little with the process.

Correlation of Incipient Boiling Data

An incipient boiling data correlation can be obtained directly from figures 2 and 5 by inspection and definition. The nonboiling condition is represented by a value of heat transfer coefficient ratio equal to unity and the boiling condition by the 0.7 slope line. The intersection of these lines is defined as the incipient boiling point; for both cryogens it occurs at a value of the dimensionless parameters of 0.0014.

The incipient boiling correlation for both liquid nitrogen and liquid neon can be represented by the equation*

$$\left(\frac{q\rho_{(bx_i)}}{\lambda G \rho_v}\right)\left(\frac{\lambda}{H_s - H_{(bx_i)}}\right)^{1.2}\left(\frac{\rho_v}{\rho_l}\right)_s^{1.4} = 0.0014 \qquad (6)$$

For a given q, $\dot{\omega}$, and system pressure level, to solve equation (6) for bulk enthalpy at the incipient boiling point requires an iteration technique since both bulk enthalpy $H_{(bx_i)}$ and bulk density $\rho_{(bx_i)}$ are unknowns.

Position of Boiling Incipience

In a flow channel subjected to uniform convective heat fluxes, different modes of heat transfer can exist simultaneously at different locations along the channel, and the transition position can be stable. For the transition from forced convection to nucleate boiling the position of boiling incipience (x_i) in a tube can be determined by the relation

---

*The apparent insensitivity of eq. (6) to temperature difference follows from the data. A given heat flux and pressure level fixes the wall temperature at boiling incipience.

$$x_i = \frac{\dot{\omega}}{qhd}\left(H_{(bx_i)} - H_{in}\right) \tag{7}$$

where equation (6) is used to calculate $H_{(bx_i)}$.

The liquid nitrogen and liquid neon data obtained for this study were used to calculate the position of boiling incipience over a wide range of test conditions. Experimental values of the position of boiling incipience were obtained from temperature profiles plotted as in figure 8; this figure shows the liquid nitrogen data at a system pressure of 2.17 MPa (21.7 bars) and a flow rate of 6.8 g/sec for three different heat fluxes.

Whether nonboiling or boiling exists is evident from the slope of the lines drawn through the plotted points. The linear relationship between increasing wall temperature and heated length is typical of forced convection heat transfer data. Boiling occurs when the wall temperature is some finite value greater than the saturation temperature of the fluid which in figure 8 equals a superheat of 3 K. After boiling starts the wall temperature remains constant along the tube as long as nucleate boiling persists.

The position of boiling incipience is located at the intersection of the forced convection and the nucleate boiling curves. For a heat flux of 21.2 W/cm^2, figure 8 shows that boiling incipience occurs at a heated length of 11 cm. The two lower heat flux curves are obviously nonboiling because of the monotonically increasing temperature profiles. The linear relationship between wall temperature and distance permits extrapolation to an intersection with an extension of the boiling curve. In this manner the incipient boiling point for a uniform heat flux of 16.8 W/cm^2 with the geometry used in this study was found to equal 24.6 cm of heated length and 48.8 cm for a heat flux of 11.4 W/cm^2.

The liquid nitrogen and liquid neon forced convection data and partial boiling data were treated in this manner. Comparisons were then made between the calculated and measured incipient boiling points to determine the accuracy of the calculation procedure. The results are shown in figure 9 for both experimental and extrapolated data. All data fall within a ±15 percent scatter band.

SUMMARY OF RESULTS

Liquid nitrogen and liquid neon forced convection subcooled boiling heat transfer data obtained for this study were used to develop correlations and techniques for predicting boiling incipience and convective boiling in uniformly heated flow channels. The results were obtained for the test conditions and flow geometry used in this study.

The correlation equation for the subcooled boiling data showed that, given q, $\dot{\omega}$, and bulk conditions, 82 percent of the liquid nitrogen and liquid neon data correlated to within a scatter of ±10 and ±15 percent, respectively. This is considered a reasonably minor suppression of information in the calculation of heat transfer coefficients. A comparison of calculated and experimental heat flux (q) for given ΔT, $\dot{\omega}$, and bulk conditions showed a scatter of ±30 percent for the nitrogen data and ±40 percent for the neon data. This represents considerable suppression of information, similar to that in pool boiling data.

The correlation equation for boiling incipience, solved by iterating, was used to calculate the position of boiling incipience in a flow channel subject to uniform heat fluxes. Calculated values compared to experimental data and extrapolated values showed an accuracy to within ±15 percent.

REFERENCES

1. G. M. Prok and G. V. Brown, Tech. Note D-8337(1976).

2. S. S. Papell and R. C. Hendricks, Liquid Neon Heat Transfer as Applied to a 30 Tesla Cryomagnet, presented at the Cryogenic Engineering Conference, Kingston, Ontario, July 1975, Paper #R-5.

3. L. S. Tong, Boiling Heat Transfer and Two-Phase Flow, John Wiley and Sons, Inc., New York (1965), p. 111.

4. W. M. Rohsenow and J. P. Hartnett, Handbook of Heat Transfer, McGraw-Hill, New York (1973), p. 13-1.

5. S. S. Papell, NASA Tech. Note D-1583 (1963).

6. Y. Y. Hsu, J. Heat Transfer, 84, No. 3, p. 207 (1962).

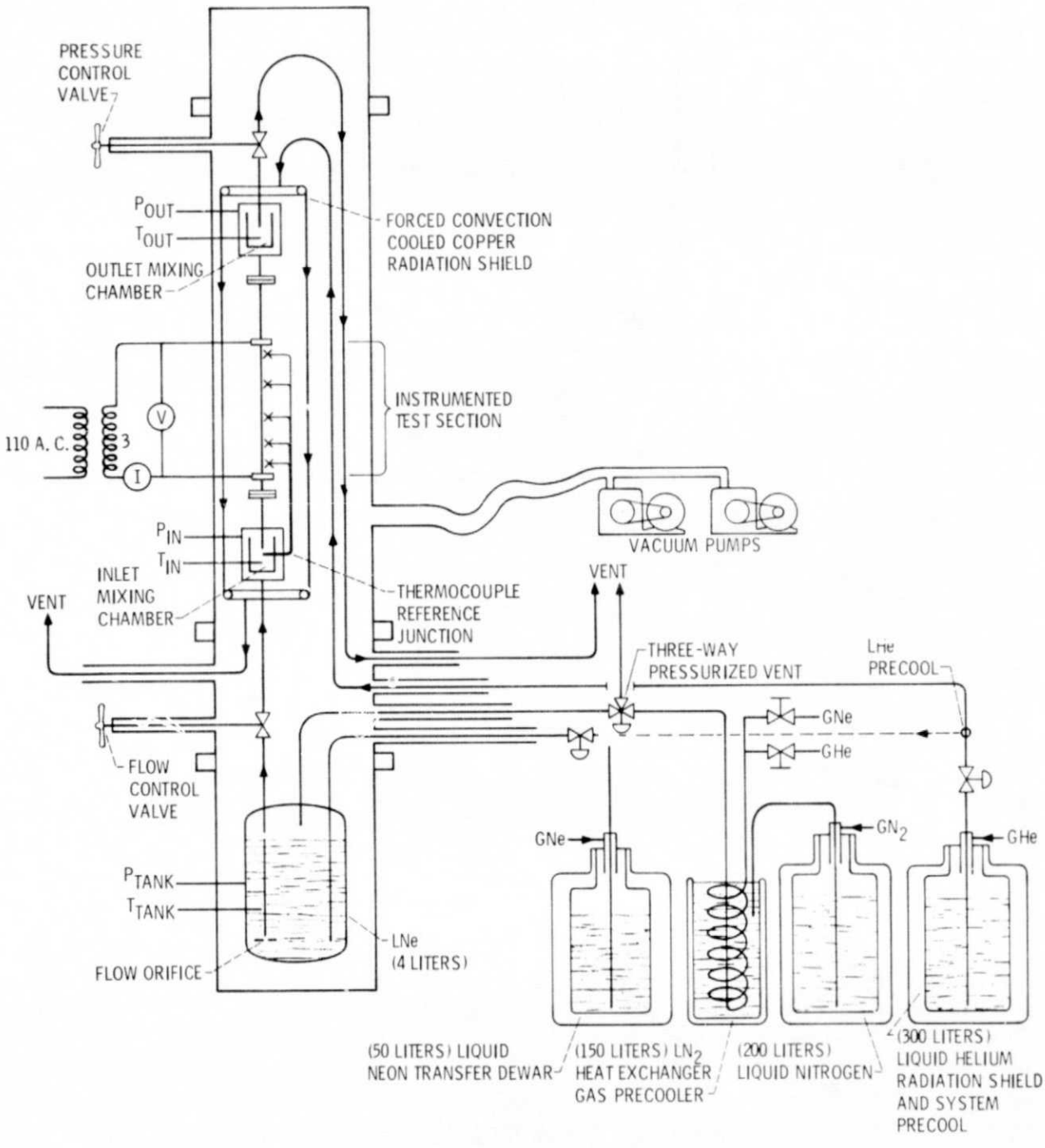

Figure 1. - Liquid neon heat transfer facility.

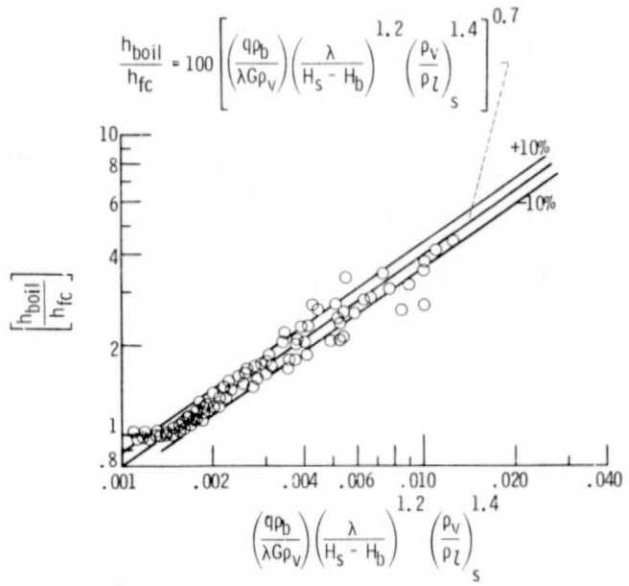

Figure 2. - Liquid nitrogen convective boiling data correlation. Pressure = 1.11 to 2.87 MPa (11.1 to 28.7 bars); flow rate = 2.7 to 6.5 g/sec; heat flux = 4.1 to 21.2 W/cm^2; subcooling = 1.5 to 26.5 K.

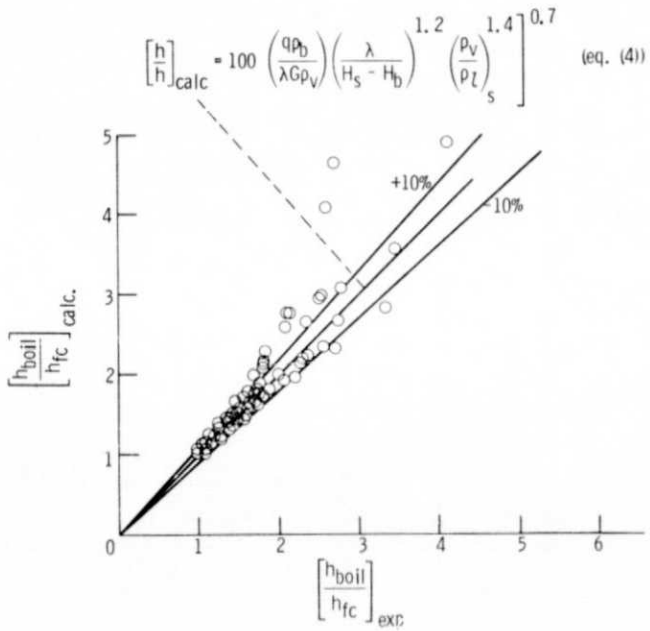

Figure 3. - Accuracy of liquid nitrogen data correlation (eq. (4)). 82 Percent of data within ±10 percent scatter.

$$q_{calc.} = \left[100\, h_{fc}\,(T_w - T_b)\right]^{3.33} \left[\left(\frac{\rho_b}{\eta G \rho_v}\right)\left(\frac{\lambda}{H_s - H_b}\right)^{1.2}\left(\frac{\rho_v}{\rho_l}\right)_s^{1.4}\right]^{2.33} \quad \text{(eq. (5))}$$

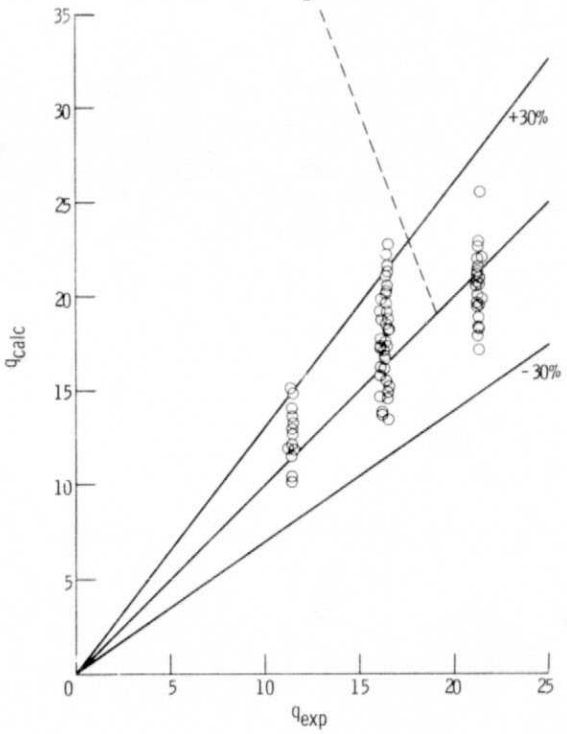

Figure 4. - Accuracy of correlation for heat flux (q) calculation using equation (5) — Liquid nitrogen data — 82 Percent of data within ±30 percent scatter.

$$\frac{h_{boil}}{h_{fc}} = 100\left[\left(\frac{q\rho_b}{\lambda G \rho_v}\right)\left(\frac{\lambda}{H_s - H_b}\right)^{1.2}\left(\frac{\rho_v}{\rho_l}\right)_s^{1.4}\right]^{0.7}$$

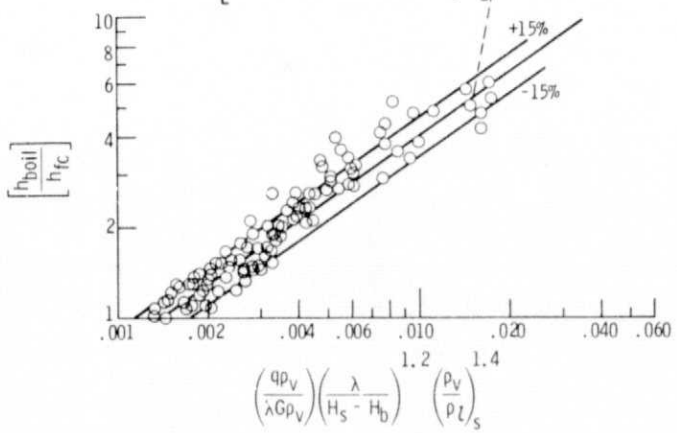

Figure 5. - Liquid neon convective boiling data correlation. Pressure = 1.12 to 1.66 MP_a (11.2 to 16.6 bars); flow rate = 4.0 t. 10.8 γ/sec; heat flux = 1.8 to 20.5 W/ cm^2; subcooling = 1.5 to 11.6 K.

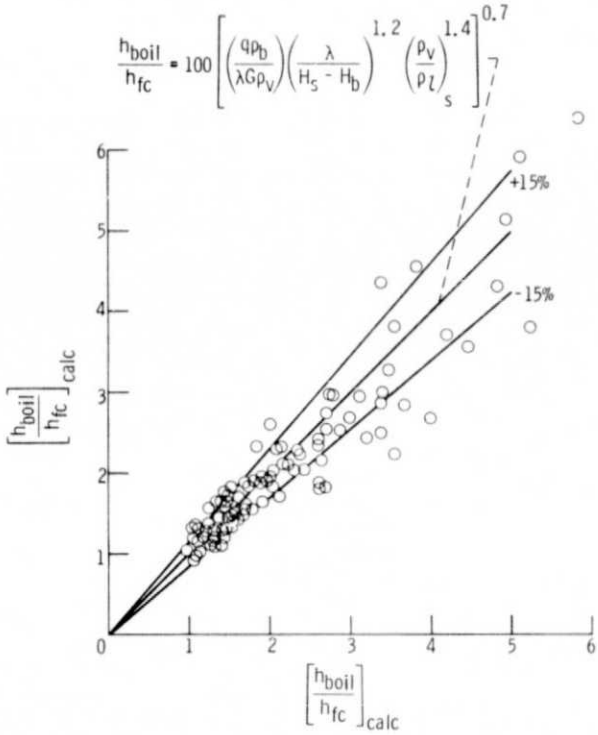

Figure 6. - Accuracy of liquid neon data correlation (eq. (4)). 75 Percent of data within ±15 percent scatter.

$$q_{calc} = \left[100\, h_{fc}\,(T_w - T_b)\right]^{3.33}\left[\left(\frac{\rho_b}{\lambda G\rho_v}\right)\left(\frac{\lambda}{H_s - H_b}\right)^{1.2}\left(\frac{\rho_v}{\rho_l}\right)_s^{1.4}\right]^{2.33} \qquad \text{(eq. (5))}$$

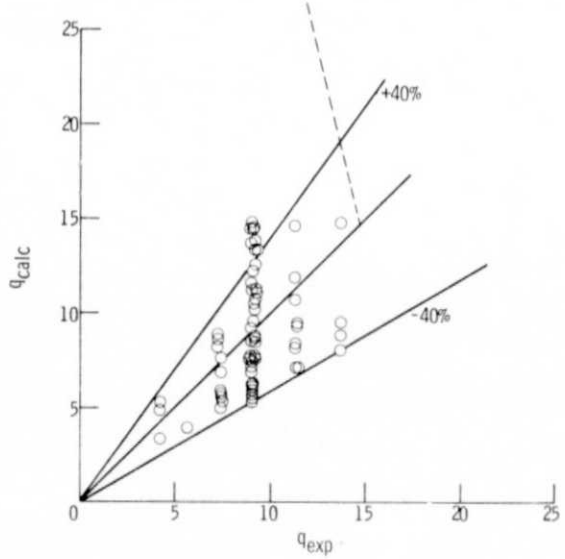

Figure 7. - Accuracy of correlation for heat flux (q) calculation using equation (5). Liquid neon data – 75 percent of data within ±40 percent scatter.

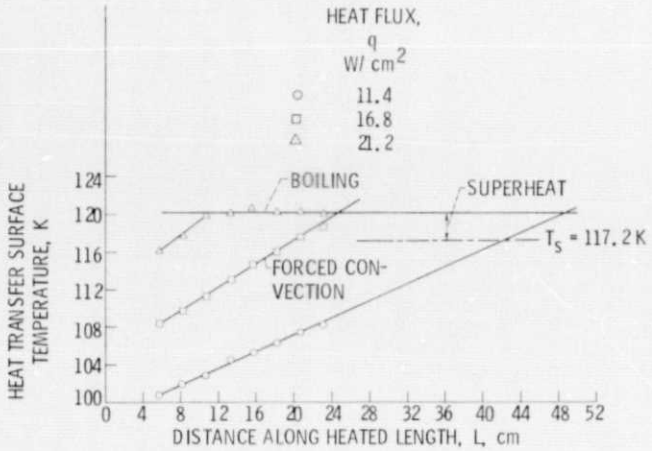

Figure 8. - Test section tube wall temperature profile data for liquid nitrogen at a system pressure of 2.17 MPa (21.7 bars) and a flow rate of 6.8 g/sec.

$$\left(\frac{q\rho_{(bx_i)}}{\lambda G \rho_v}\right)\left(\frac{\lambda}{H_s - H_{(bx_i)}}\right)^{1.2}\left(\frac{\rho_v}{\rho_l}\right)_s^{1.4} = 0.0014 \quad \text{(eq. (6))}$$

$$x_i = \frac{\dot{\omega}}{q\pi d}\left[H_{(bx_i)} - H_{in}\right] \quad \text{(eq. (7))}$$

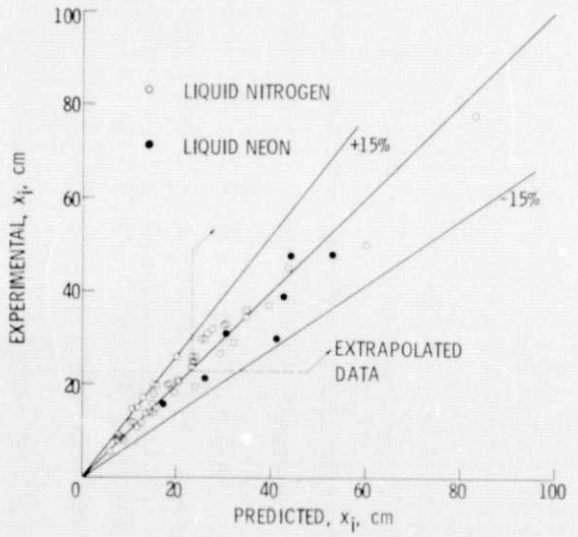

Figure 9. - Accuracy of calculation procedure for predicting the position of boiling incipience (x_i) in a uniformly heated tube using equations (6) and (7).